



# Journal of Materials and Engineering Structures

## Research Paper

### Strengthening of Self-Consolidating High Strength RC Dapped Ends with CFRP Fabrics

Qasim M. Shakir \*, Baneen B. Abd

University of Kufa, Faculty of Engineering, Najaf, Iraq

#### ARTICLE INFO

##### Article history :

Received : 11 May 2018

Revised : 28 June 2018

Accepted : 29 June 2018

##### Keywords:

Dapped ends

Self-consolidatingg

STM model

CFRP Fabrics

#### ABSTRACT

In this work, an experimental study has been conducted to investigate the behavior of self-consolidating high strength reinforced concrete dapped end beams upgraded with CFRP composites. A series of 14-specimens have been tested, each of with length of 1500 mm, total depth of 400mm and width of 200mm. Two values of shear slenderness ratio ( $a/d$ ) namely (1.5 and 1.0) are adopted. Two specimens have been considered as a reference beams (with full Design reinforcement), four were deficiently reinforced in either hanger or the extended disturbed zone, and the other eight beams have been upgraded with a variety of arrangements by CFRP fabric. This work aims to observe the effects of deficiently reinforced disturbed zones on the resistance and overall behavior of such elements. Also, the extent of strength recovery using CFRP sheeting. It is observed that reducing the hanger reinforcements by a half, results in a drop of capacity by (13%) regardless of values of ( $a/d$ ). Furthermore, it is noticed that adopting the inclined arrangement of CFRP sheets with ( $45^\circ$ ) yielded the best results if compared with other arrangements. An enhancement in failure load was about (23%) for ( $a/d=1.0$ ).

## 1 Introduction

Precast concrete appeared in the last century, its use has increased dramatically because of its many known features. This type of industry depends on the regular casting of pieces of concrete and then linking them to the site. There was a need to address the points of linkage between the various elements, such points are called connections. A connection is one of the essential parts of precast concrete that should be given a considerable attention when dealing with such type of structures to insure that the load is transferred across it without local failure. The corbels and beams with Dapped-end (DEB) are the most used forms to constitute the connections [1]. The present study is concerned with the high strength concrete dapped ends. The dapped-end beams are the precast RC beams with reduced depth at end. However, as the flow of internal forces is interrupted by the sudden change in geometry, regions of disturbances in the flow of these forces are created around the re-entrant corner and in the nib. These regions are referred to as "disturbed regions". For analysing and

\* Corresponding author. Tel.: +964 7832460562.

E-mail address: qasimm.alabbasi@uokufa.edu.iq

designing disturbed regions of the dapped end beam, Strut and Tie Model (STM) may be utilized, which are idealized using an inclined compressive strut in the nib, and compressive struts radiating from the bottom corner of the beam, or can be designed by any appropriate method rather than the ordinary flexural analysis theory (Bernoulli theory) [2,3].

The design of connections of dapped-end is a paramount aspect in a precast concrete industry although its analysis become a complicated problem. They may be subjected to high stresses as well as to unforeseen forces such as temperature changes. The dapped end beam provides an efficient and economical connection of precast to precast or precast to cast-in-place concrete components. The connection has several economic advantages such as: the cost of material used for the connection is reduced by eliminating all miscellaneous steel inserts and welding. The connection is normally located at the point of inflection, thus the moment and corresponding flexural reinforcement are reduced. The dapped end beam connection may have wide practical application such as drop-in beam between two corbels, a drop-in beam between two cantilever beams, a connection between joist to beam and a connection between beams to column [1].

Besides use of dapped end is to get a better fabrication with columns in connection, they are also used to reduce overall height of the structure and increase stability for load bearing support. They are very commonly used in reinforced concrete structures such as precast buildings, parking structures and recently in precast strap footings as it furnishes greater lateral stability and minimize the floor height; also, they are frequently found in bridge girder [4]. The concept of designing RC corbels was extended and applied for the first time on dapped ends, by Mattock and Chan [5]. Eight full-scale specimens were tested; four under the effect of vertical load only, and others were under a combined action of vertical and horizontal loading. It was concluded that the dapped end could be considered as an inverted corbel with adding the hanger reinforcement. The shear span ( $a$ ) to be used equals to the distance from the centre of hanger reinforcement to the support reaction. So [2] tested two thin stemmed beams having dapped end beams with different geometries and reinforcement by using Strut and Tie Model (STM). Results showed that STM models were able to estimate the failure load of dapped end. He found a notably improve in ductility of the dapped end when two layers of symmetrically placed welded wire fabric had been used, which served as the shear reinforcement in the region of uniform compressive stress fields. Also, a comparison between the inclined dapped end with the rectangular one was done. Through a series of experimental tests of 24 dapped end specimens, Wang et al.[6] studied several parameters that may affect the behaviour of such elements which were the dapped end height, the bent form of the longitudinal reinforcement and distance from the re-entrant corner, at which the hanger stirrups to be distributed. They reported that the first crack was always initiated at the re-entrant corner of the dapped end with angle ( $40^{\circ}$ - $60^{\circ}$ ). Furthermore, it was reported that the angle of alignment of the hanger stirrups with respect to the vertical axis and using bent ends for the longitudinal reinforcement has significant influence on the shear strength and failure load if compared with the conventional stirrups with closed and vertical alignment. Regarding dimensions of the dapped ends, it was found that the height of the nib affecting significantly on shear capacity. It was concluded that the height of the nib end should be larger than  $0.45h$  (full depth of the beam) and the effective range of the hanger stirrups was proposed to be one-half the full depth of dapped end. Peng T., [7] investigated two dapped end beams with different reinforcing details to study the behavior of disturbed regions. The parameters studied was the anchorage of the hanger and the flexural reinforcement. STM models was used for the design and strength predictions. The results showed that the design using STM models for dapped/end beams provides a conservative approach, and the anchorage and the details of hanger steel and longitudinal reinforcement have greatly influenced the shear capacity and ductility. S.E.-D.M.F. Taher, [8] tested 52 dapped ends to study the strengthening of dapped ends. Different techniques were used such as bonding of steel angle at the recess corner, unbonded inclined steel bolt anchors in pre-drilled hole, external steel plate jacketing, exterior carbon fibre wrapping within the beam stem, exterior CFRP stripping and combination of carbon fiber wrapping and strapping to determine the best strengthening method. A comparison was conducted with the STM model, and It was reported that the mode of failure was mainly effected by the introduced reinforcement detailing defect in the recess zone. It was recommended that externally bonded FRP retrofitting systems constituted a viable solution in upgrading, or repairing fields and it provides ease fabricated horizontal carbon fibre wrapping in both the reduced and full depth zones with inclined CFRP stripping. Tests on full-scale dapped ends have been achieved by Amir W. et al.,[9]. Ten prestressed concrete beams having Tee-cross section have been investigated. Several configurations of hanger reinforcements were studied which were; the L-, Z-, C-, and CZ- shapes with vertical alignment, inclined L- shaped and welded wires (BRC) reinforcement. Several parameters that may have a considerable impact on behavior of dapped end were discussed, including the effect of restressing of the nib and splice length of the hanger reinforcement. Several conclusions were addressed as that crack propagation at service loading might be restricted by extending the prestressed steel through the nib and using inclined L- shaped hanger steel enhanced response considerably in comparison with other arrangements. This may be explained as that hanger steel is closely parallel to the orientation of diagonal tension.

## 2 Experimental program

In the present work, an experimental study has been conducted to observe the performance of high strength self-consolidating (SCC) reinforced concrete dapped ends. The program comprised of monitoring the behaviour of 14 specimens with detail shown in Fig.(1). Two values of shear slenderness ratio ( $a/d$ ) which are 1.5 and 1.0 are used. This work aims to discuss effect of shear slenderness ratio on the response of dapped ends, range of ability to retire strength in the deteriorated members (expressed here in terms of internal deficiencies) and investigate the best alignment of CFRP fabrics to be installed when using in strengthen and rehabilitation. All beams were tested under the effect of one point static loading at the Structural Laboratory in the Department of Civil Engineering / Faculty of Engineering / Kufa University.

## 3 Materials properties

The properties of all materials, which used in the SCC concrete mix of the beam specimens, are presented. These materials are cement, water, coarse aggregate (gravel), fine aggregate (sand), limestone powder, super plasticizer, steel bars and CFRP fabrics.

### 3.1 Cement

In this study, ordinary Portland cement (OPC), Type I, which is produced by (KAR) company for cement production (Najaf- Iraq) has been used. The product has been tested to conform the requirements of the Iraqi Specifications (IQ.S. 5/1984)[10]. The chemical and physical analyses of this cement are shown in Tables (1) and (2) respectively.

**Table 1-Chemical Composition of Cement**

Compound Composition	Chemical Composition	Percentage By Weight %	Limit Specification
Lime	CaO	62.20	-
Silica	SiO <sub>2</sub>	22.42	-
Alumina	Al <sub>2</sub> O <sub>3</sub>	2.1	-
Iron oxide	Fe <sub>2</sub> O <sub>3</sub>	4.4	-
Magnesia	MgO	2.40	5.0 (Max.)
Sulfate	SO <sub>3</sub>	2.40	2.8 (Max.)
Loss on ignition	L.O.I.	3.4	4.0 (Max.)
Insoluble residue	I.R.	0.99	1.5 (Max.)
Lime saturation factor	L.S.F.	0.87	(0.66-1.02)

**Table 2-Physical Properties of the Cement**

Physical Properties	Test Result	Limit of IOS 5:1984
Fineness using Blaine air permeability apparatus(m <sup>2</sup> /Kg)	291	230 (Min.)
Soundness using autoclave method (%)	0.47	0.8 (Max.)
Setting time using Vicat's apparatus		
Initial (min)	1:10	45 (Min.)
Final (hr)	4:35	10 (Max.)
Compressive strength for mortar cube (70.7 mm) at		
3 days (MPa)	19.28	15 (Min.)
7 days (MPa)	30.44	23 (Min.)

### 3.2 Water

Potable tap water is used for concrete mix, washing sand and gravel particles, and curing for all specimens.

### 3.3 Fine Aggregate

Normal sand imparted from Al-Najaf zone – Iraq, was used as fine aggregate for concrete mixing in the present work. The maximum size of sand was (10mm) with specific density of (2.56). The grading of this sand within zone 2 is depicted in Table (3). Table (4) shows physical properties of the fine aggregate. The tests result was obtained satisfying the requirements of (IQS limits No.45/1984)[11].

**Table 3- Grain Size Distribution of Fine Aggregate**

Sieve Size	% Passing	
	Fine Aggregate%	IQS limits No.45/1984 ( Zone 2)
10 mm	100	100
4.75 mm	100	90-100
2.36 mm	96	75-100
1.18 mm	82	55-90
0.60 mm	56	35-59
0.30 mm	16	8-30
0.15 mm	8	0-10

**Table 4-Physical Properties of Fine Aggregate**

Physical Properties	Test Results	Limit Specification
Specific density	2.56	–
Sulfate content	0.09 %	≤ 0.5 %
Absorption	0.73 %	–

### 3.4 Coarse Aggregate

Crushed coarse aggregate of maximum size (20mm) with absorption and specific density (0.75%) and (2.6) respectively is used for casting all concrete samples. Sieve analysis test shows that the coarse aggregate gradation conform the requirements of the Iraqi specifications (IQ.S.45/1984)[11]. Table (5) shows the grain size distribution and Table (6) shows the physical properties of the coarse aggregate used in the SCC mix.

**Table 5- Grain Size Distribution of Coarse Aggregate**

Sieve Size (mm)	% Passing	
	Coarse Aggregate	Limit Specification
20	100	95-100
14	86.45	80-90
10	44.26	30-60
5	2.42	0-10

**Table 6- Physical Properties of Coarse Aggregate (Gravel)**

Physical Properties	Test Results	Limit Specification
Specific density	2.6	–
Sulfate amont	0.06%	≤ 0.1%
Absorption	0.75%	–

### 3.5 Limestone Powder(LSP)

Limestone powder (which has a local name as Al-Gubra) used in concrete mixes serves as a filler material and has several functions that contribute in producing SCC mixes.it is used to increase quantity of fines, restrict generating large amount of heat of hydration , improving flow and cohesion characteristics and increase resistance to segregation. The grain size distribution of Al-Gubra(LSP) conform to EFNARC [12] and the chemical compositions are listed in Table (7).

**Table 7- Chemical Compositions of (LSP) [12]**

Oxides		%
Calcium oxides	CaO	54.1
Silicon oxides	SiO <sub>2</sub>	1.38
Aluminum oxides	Al <sub>2</sub> O <sub>3</sub>	0.72
Ferric oxides	Fe <sub>2</sub> O <sub>3</sub>	0.12
Magnesium oxides	MgO	0.13
Sulphur trioxides	SO <sub>3</sub>	0.21
Loss on Ignition	L.O.I	42.56

### 3.6 Superplasticizer

Super Plasticizer type GLENIUM®54 is used in the present work [13]. The characteristics of the superplasticizer are listed in Table (8).

**Table 8-Properties of Superplasticizer[13]**

Commercial Name	Glenium 54
Form	Viscous liquid
Color	Light brown
Relative density	1.08 – 1.15 g/cm <sup>3</sup> @ 25° C
PH	6.6
Viscosity	128μ 30 cps @ 20° C
Transport	Not classified as dangerous
Labeling	Not hazard label required
Chlorides	Free from chlorides

### 3.7 Steel Reinforcing Bars

Steel bars used consists of three sizes of deformed bars. Bars with diameter of 16 mm served as main longitudinal reinforcement of the beam and nib end, 10mm diameter bars served as hanger stirrups and 12mm bars to resist tension within the hanger zone. The materials properties for tested steel bars are listed in Table (9). The tests were conducted on the Engineering Consulting lab at University of Kufa according to ASTM A370-2005 specifications [14].

**Table 9-Properties of Steel Bars**

Nominal Bar Diameter (mm)	Measured Bar Diameter (mm)	Yield Stress* (MPa)	Ultimate strength* (MPa)
10	9.8	568	726
12	11.89	615	712
16	16.08	634	748

\* Value expresses the average of three test specimens with length 50 cm. each.

### 3.8 Carbon Composite Strips (CFRP)

CFRP fabric of the type SikaWrap®-301C which has (0.167mm) thickness, (50mm) widths and tensile strength (4900MPa)[15]. The epoxy based impregnating resin of type Sikadur-330 with tensile strength (30MPa)[16] is adopted in retrofitting of the zones in the dapped ends that include some internal reinforcement deficiencies.

### 3.9 Self-Consolidating Concrete Mix Proportions

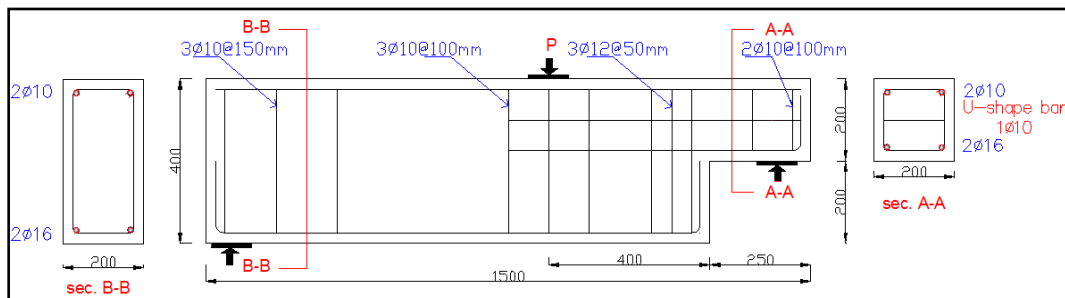
Several trial mixes have been tested to produce a self-consolidating mix with 150mm cube concrete strength of 51 MPa. The SCC mix design is based on the ACI committee [17] to satisfy the requirements of workability, fluidity and resistance to segregation. Table (10) indicates the quantities of the constituent materials of the mix adopted in present work.

**Table 10- Proportions of Concrete Mix**

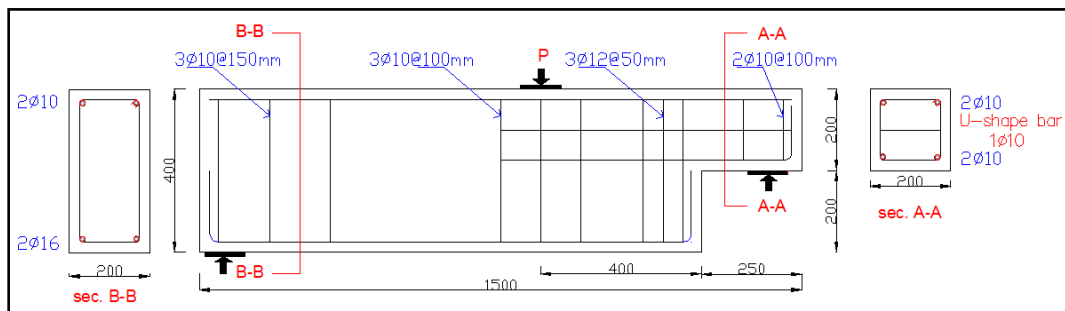
Material	Quantity
Cement (kg/m <sup>3</sup> )	400
Fine Aggregate (kg/m <sup>3</sup> )	962
Course Aggregate (kg/m <sup>3</sup> )	780
Limestone Powder (kg/m <sup>3</sup> )	75
Water (kg/m <sup>3</sup> )	128.7
Water/ Cement Ratio	0.32
Superplasticizer (L/m <sup>3</sup> )	4.8

**4 Description of Specimens**

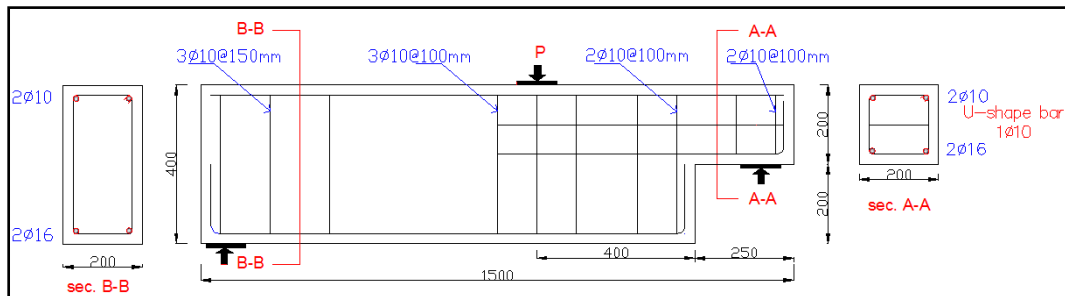
For all specimens, the cross section dimensions were (200mm) width , (400mm) height, and the overall length was (1500mm). The nibs had a length of (250mm) and an overall depth of (200mm). The specimens have been grouped into two categories (A and B). For both categories, one specimen served as a reference beam, two with reduced reinforcement in either hanger or nib zones and other four beams are strengthened with CRFP sheets. For group A, the (shear span/ effective depth) ratio (also called shear slenderness ratio) is (a/d=1.5) and for group B, slenderness ratio is considered to be (1.0). The dimensions and reinforcement detailing for typical specimens are shown in Fig. 1.



(a) Details of Loading and Reinforcement for Control Beam



(b) Details for Nib Reduced Reinforcements Beam



(c) Detail of the Hanger Reduced Reinforcements Beam

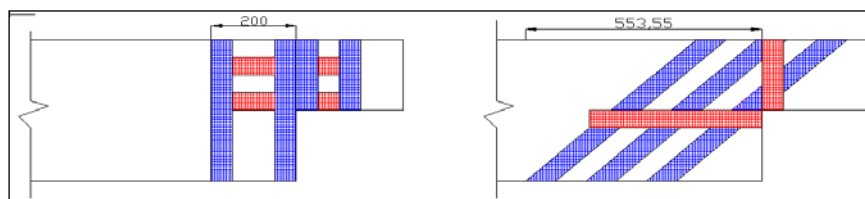
**Fig. 1- Details of Reinforcement Beams**

### 5 CFRP Strengthening Systems

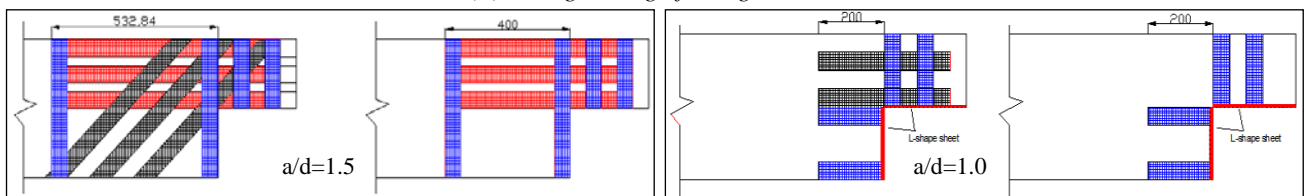
The arrangements suggested to retrofit the specimens with internal deficiencies are chosen closely based on the trends of cracking propagation of the reference beams, the ability to achieve the strengthening with few difficulties and practical requirements. This work consists strengthening of eight dapped ends with externally bonded (CFRP) fabrics as stated in Table (11), and depicted in Fig. (2). The procedure can be summarized as follows: the reference beams are tested first, the failure modes are determined and the trend of crack propagation was traced. Then, the first configuration of strengthening is installed and the beam is tested. Based on the results of the first scheme, the second arrangement is proposed, and so on.

**Table 11- Characteristics of Beams Tested and Parameters Investigated**

Symbol Beams	CFRP Properties
CONT-A	Full reinforcement
HCONT-A	The hanger reinforcement is reduced by 50%
HSTR-1-A	3-strips with angle 45 <sup>0</sup>
<b>Group-A</b> <b>a/d= 1.5</b>	
HSTR-2-A	2-vertical U-shape in hanger and nib+ 2-horozotal strips in nib face
NCONT-A	The nib reinforcement is reduced by 60%
NSTR-1-A	L-shaped sheet 1-layer
NSTR-2-A	L-shaped sheet 1-layer + 2-horozotal sheet in each face
CONT-B	Fill reinforcement
HCONT-B	The hanger reinforcement is reduced by 50%
HSTR-1-B	3-strips with angle 45 <sup>0</sup>
<b>Group-B</b> <b>a/d= 1.0</b>	
HSTR-2-B	2-vertical -U-shape in hanger and nib + 2-horozotal strips in nib face
NCONT-B	The nib reinforcement is reduced by 60%
NSTR-1-B	3-horizontal strips in nib face + 2-vertical U-shape in hanger
NSTR-2-B	3-horizontal strips in nib face +3-strips with angle 45 <sup>0</sup>



(a) Strengthening of Hanger Zone



(b) Strenthening of Nib Zone

**Fig. 2- Details of Strengthening of Dapped end Beams**

### 6 Test setup

The universal machine in the Structural Lab./University of AL-Kufa is used to achieve the tests, with maximum capacity of 200 ton. The tested specimen is supported on roller from one end and hinged from other end with c/c spans of

1260mm and 1340 for shear slenderness ratio 1 and 1.5 respectively, Steel bearing plate of (100x200x10 mm) are used at supports and loading point to distribute the concentrated forces. A typical specimen is loaded with one-point load at a distance equals to the overall depth of the beam. A dial gauge with accuracy 0.05mm is located under the loading point to record the vertical deflection with progress in loading.

## 7 Experimental results

In this section, results of the experimental work that is devoted to study effect of lack of amount of reinforcements in hanger and nib zone, effect of the shear slenderness ratio and behavior of strengthening configurations by CFRP strips in both regions on the overall response of dapped end beams.

In all control beams, the first cracks initiated at the corner of dapped end beam, while in strengthened beams, the flexural shear crack was the first crack occurred at mid span of the beam with vertical or diagonal trend toward the point load.

The first crack load, failure load, failure patterns and deflection at final stage of loading are listed in Table (12). The discussion of results obtained for specimen is presented in the following sections.

**Table 12- First crack Loads, Failure Loads and patterns for the Tested Specimens**

(a/d) Ratio	Specimens	Shear Cracking* Load (kN)	Flexural** Cracking Load (kN)	Ultimate Load Pu (kN)	Max. Deflection (mm)	Failure Mode
<b>Group-A</b> a/d= 1.5	CONT-A	40	97	285	10.33	Diagonal shear failure in the extended end
	HCONT-A	35	75	248	9.88	Diagonal shear failure in the extended end
	HSTR-1A	175§	75	300	8.9	Diagonal shear failure at the far side of dapped end
	HSTR-2A	125§	50	280	8.11	Diagonal shear failure at the far side of dapped end
	NCONT-A	25	95	182	5.77	Direct shear failure at re-entrant corner
	NSTR-1A	35§	75	185	4.28	Diagonal failure at the re-entrant corner+ rupture L-sheet
	NSTR-2A	50§	80	200	3.82	Diagonal failure at the re-entrant corner+ delamination
<b>Group-B</b> a/d= 1.0	CONT-B	50	100	300	7.44	Diagonal shear failure at the re-entrant corner
	HCONT-B	25	70	262	7.05	Diagonal shear failure in the extended end
	HSTR-1B	120§	75	340	6.4	Delamination of inclined CFRP sheet at the top of the extended end
	HSTR-2B	100§	70	320	7.8	Rupture of CFRP sheet at the full-depth
	NCONT-B	20	90	255	8.1	Diagonal shear failure near the extended end
	NSTR-1B	80§	70	295	6.88	Flexural failure at mid span
	NSTR-2B	100§	75	300	5.58	Flexural failure at mid span

\*At re-entrant corner    \*\*At mid span    § :As observed

**7.1 Control Specimens (CONT-A & CONT-B)**

These specimens are reinforced with full reinforcement, (3-Φ12mm) stirrups for hanger zone and (2-Φ16mm) as tension reinforcement in nib zone to show the influence of shear slenderness ratio on load history. The results are depicted in Fig. (3), it can be concluded that adopting (a/d) value of (1.0) instead of (1.0) results in increasing the failure load capacity by about (16.6%), higher stiffness and lower deflection of about (35.5%). As well as, the pattern of failure is shifted from "diagonal tension failure at the nib end" to "diagonal tension failure at the reentrant corner", as shown in Fig. (4).

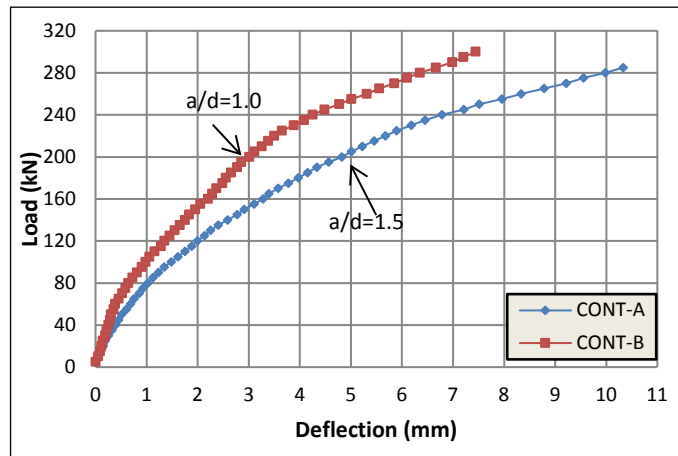
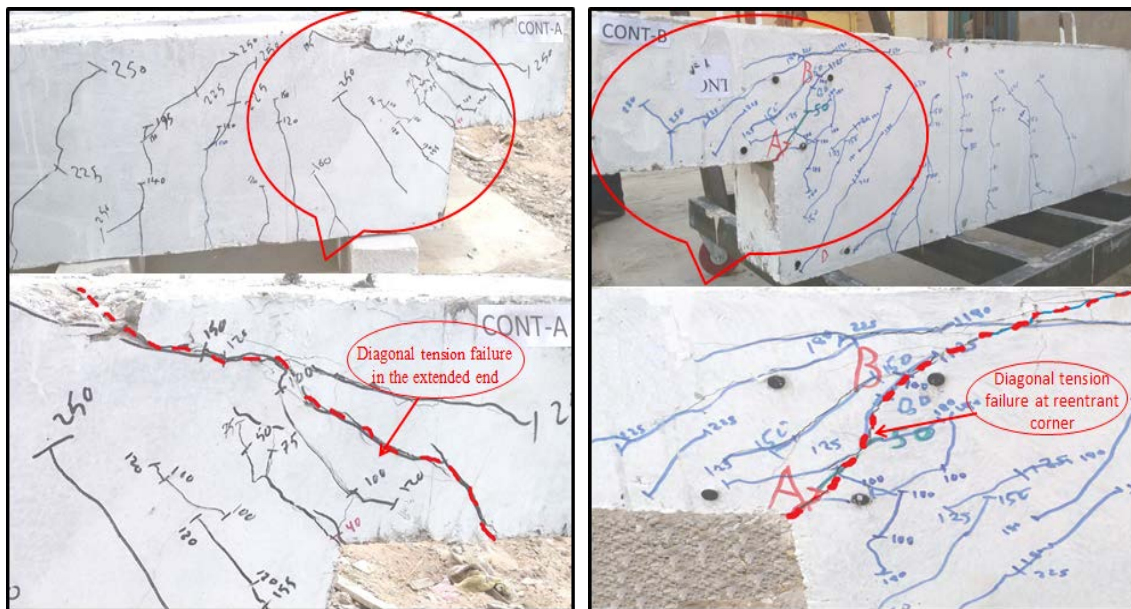


**Fig. 3- Load-Deflection Curves for Specimens with Different (a/d) Ratio**



**(a) Specimen CONT-A**

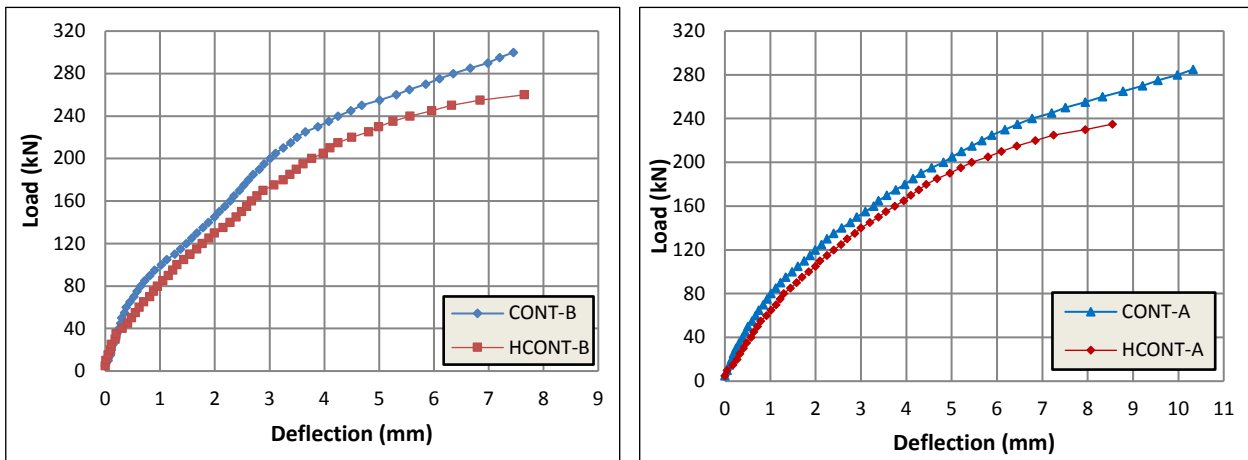
**(b) Specimen CONT-B**

**Fig. 4- Cracks Patterns for the Control Specimen (a) CONT-A (b) CONT-B**

**7.2 Specimens HCONT-A & HCONT-B**

These specimens were tested to investigate the impact of the reduction in hanger zone reinforcements on the overall behavior of the dapped end beams. All the steel of the control specimens were kept constant expect that at hanger zone were(2Φ10mm) stirrups were used (i.e. about 50% reduction).

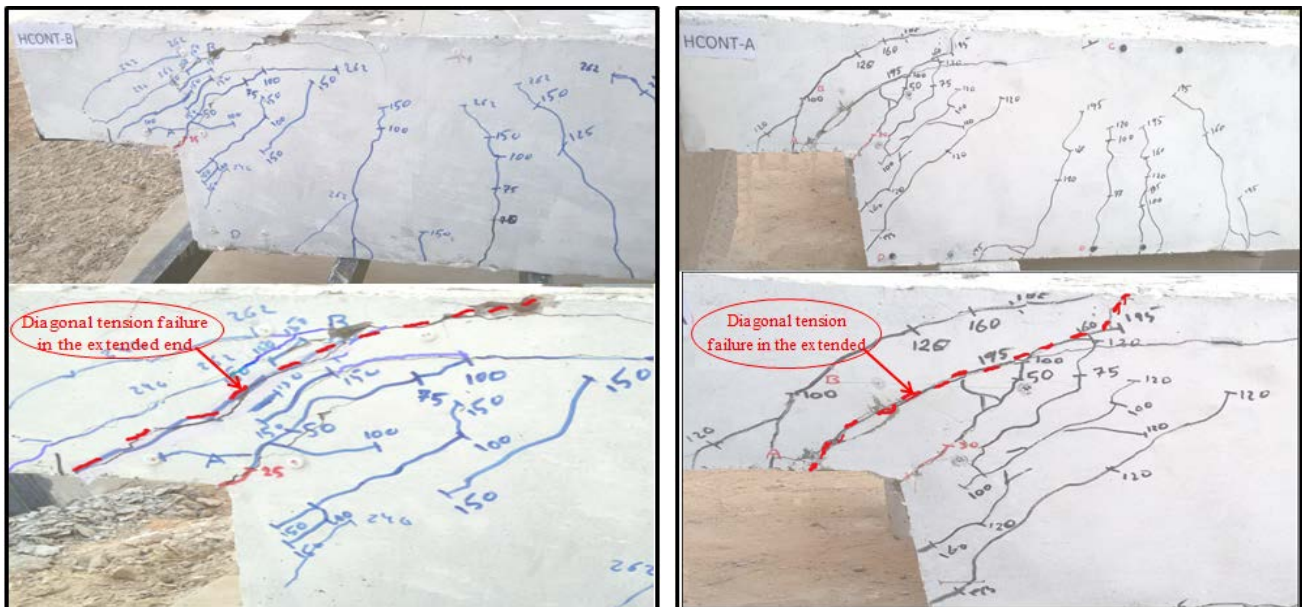
It can be noticed from Fig. (5) that the reduction in hanger reinforcement ratio results in a reduction of the failure load about (13%) for both specimens with more ductile behavior. Both specimens failed with the diagonal tension failure in the extended end, as shown in Fig. (6).



(a)  $a/d=1.0$

(b)  $a/d=1.5$

**Fig.5- Effect of Reduction Hanger Reinforcement for both  $a/d$  ratio**



(a) Specimen HCONT-A

(b) Specimen HCONT-B

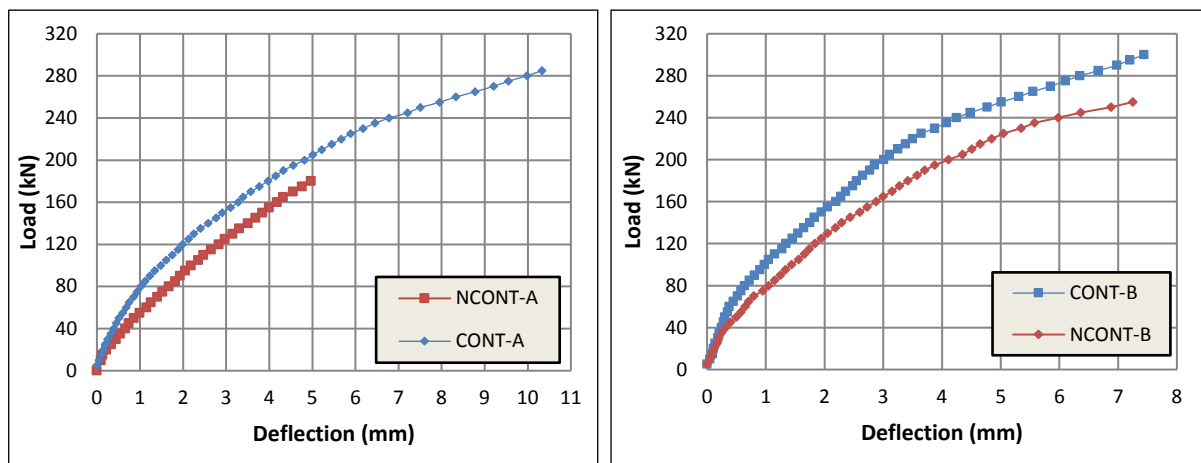
**Fig. 6- Cracks Patterns for the Specimens with Reduced Reinforcement at Hanger**

**7.3 Specimens NCONT-A & NCONT-B**

To show the effect of reduction for the nib reinforcement on the behavior of RC beams with dapped ends, specimens NCONT-A & NCONT-B have been tested with the same reinforcement of specimens CONT-A & CONT-B were adopted expect that the (2- $\Phi$ 10mm) are used as a nib reinforcement, i.e. about 60% reduction.

Figs. (7) and (8) revealed that the reduction in nib reinforcement resulted in a drop in the failure load capacity and reduction in deflection about (35.8%) and (51.88%), respectively for specimen NCONT-A( $a/d=1.5$ ). Also, it is found that

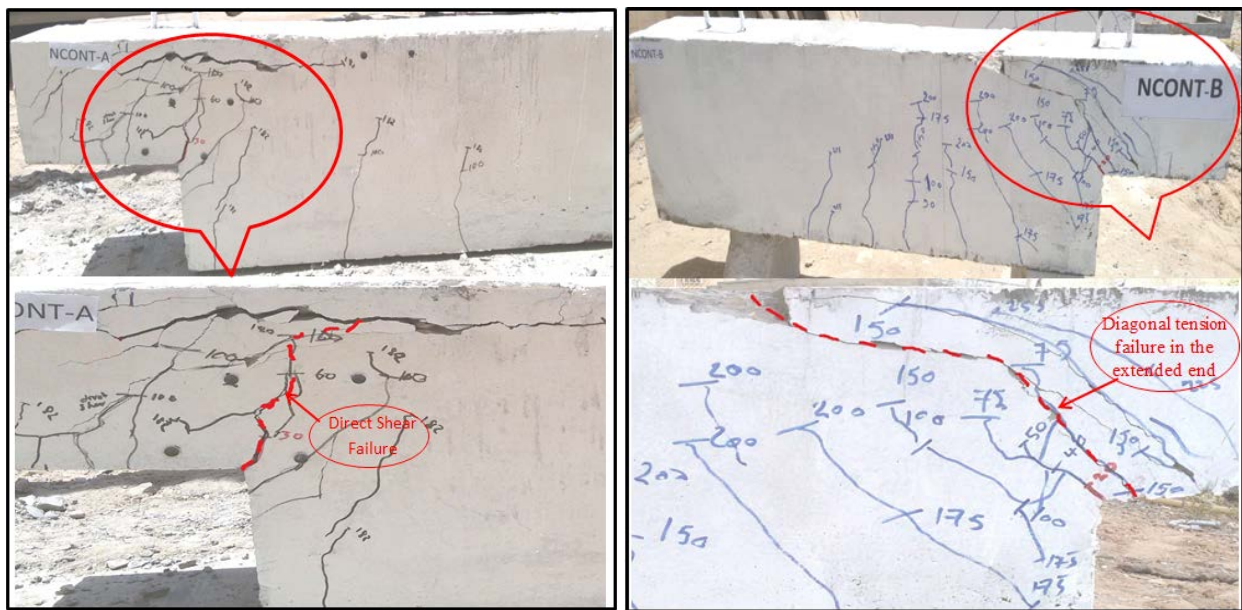
the specimen NCONT-B has a small effect of reducing the nib reinforcement of the dapped end with ( $a/d=1.0$ ), where, a reduction in the failure load and deflection about (15%) and (2.55%), respectively.



(a)  $a/d=1.5$

(b)  $a/d=1.0$

Fig. 7- Effect of Reduction Nib Reinforcement for group A & B



(a) Specimen NCONT-A

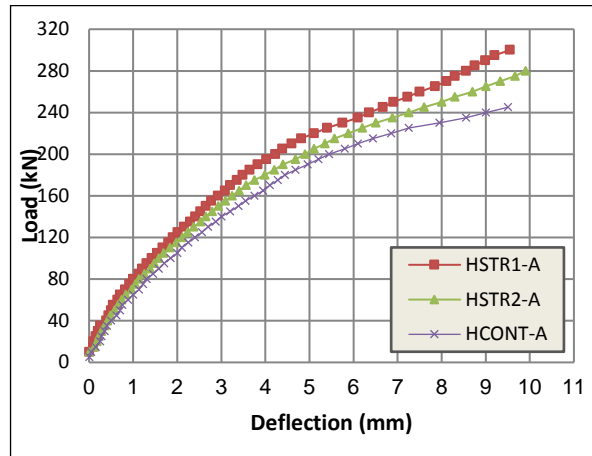
(b) Specimen NCONT-B

Fig. 8- Cracks Patterns for the Specimens with Reduced Reinforcement at Nib

#### 7.4 Specimens HSTR1-A & HSTR2-A

Two different configurations have been suggested to raise the capacity due to steel hanger reduction. The specimen (HSTR1-A) is strengthened with three strips with angle  $45^{\circ}$  to restrict the diagonal corner cracks development, while the other specimen (HSTR2-A) is strengthened with a mesh of two horizontal and four vertical strips.

Fig. (9) shows the load history obtained for the two retrofitted specimens relative to the specimen (HCONT-A). It can be seen that the specimen (HSTR1-A) yielded stiffer response and higher load capacity than the (HSTR2-A), i.e. an increment in the failure load capacity about (17.33% and 11.43%) with respect to (HCONT-A), respectively.



**Fig. 9- Effect of Strengthening Hanger Region on response ( $a/d=1.5$ )**

Comparing the crack patterns for specimens (HSTR1-A) and (HSTR2-A) with the specimen (HCONT-A). It can be seen almost few cracks formed in the extended end and hanger regions. Also, a change in mode of failure to diagonal shear flexural failure in the far part of beam while it was diagonal tension failure in the extended end for beam (HCONT-A), because of the presence the CFRP sheets which results in shifting cracks far away towards the mid span of the beam, as shown in Figs. (10) and (11).

It can be observed, the cracks near the strengthened region widened slightly and propagated in far part from the loading point, which it grow rapidly led to failure of specimens. It obviously can be concluded that more load capacity could be recorded, when using stirrups in mid span of beam.



**Fig. 10- Cracks Pattern for the Specimen HSTR1-A**

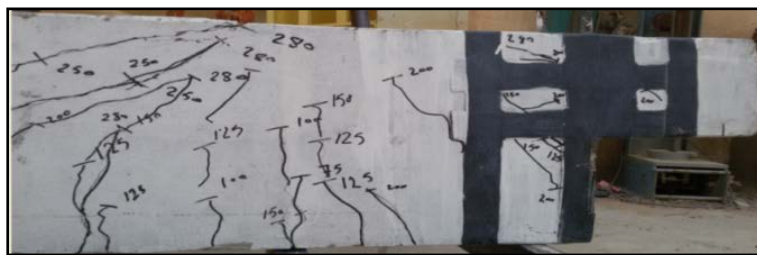


**Fig. 11- Cracks Pattern for the Specimen HSTR2-A**

**7.5 Specimens HSTR1-B & HSTR2-B**

The same strengthening configurations are used for corresponding specimens with ( $a/d=1.5$ ). Compared with specimen (HCONT-B), it can be noticed that the failure load was increased of about (23.23% and 18.43%), respectively, as shown in Fig. (12).

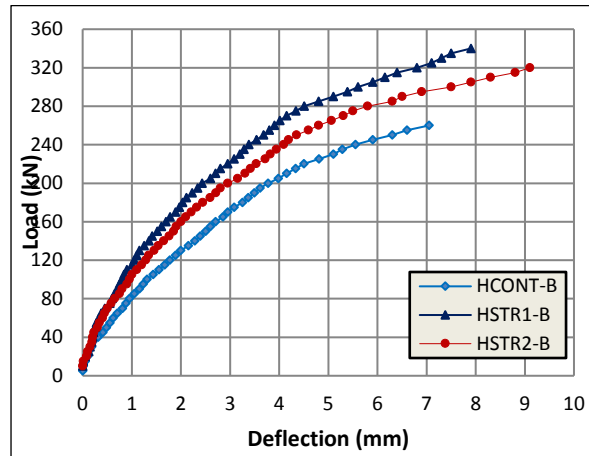


**Fig. 12- Effect of Strengthening Hanger Region on response ( $a/d=1.0$ )**

Regarding the cracks patterns of these strengthened specimens when compared to specimen (HCONT-B), few cracks were observed in the extended end and hanger regions, and cracks didn't penetrate through the (CFRP) sheets. Thus, led to a shifting of cracks away from the strengthened region and the failure of the strengthened specimens occurred due to rupture of the (CFRP) sheets, as shown in Figs. (13) and (14).



**Fig. 13- Cracks Patterns for Strengthening of beam HSTR1-B**



**Fig. 14- Cracks Patterns for Strengthening of beam HSTR2-B**

**7.6 Specimens NSTR1-A & NSTR2-A**

These specimens were strengthened with L-Shaped CFRP sheets at lower face of the nib end; the (NSTR2-A) has the same strengthening configuration as the (NSTR-1A), with adding two strips that are horizontally aligned at each side of the dapped end to increase shear strength at the reentrant corner.

Comparing the load-deflection curve of these specimens against the specimen (NCONT-A), it can be noticed, that the maximum load capacity is improved by about (2.7% and 10%), respectively, and the deflection is decreased by about (23% and 34%), respectively, as shown in Fig (15).

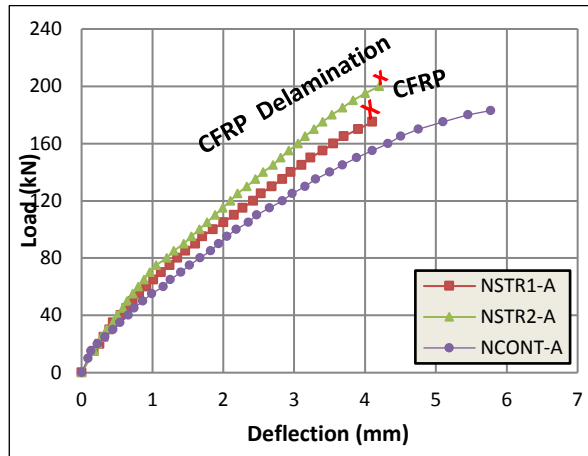


Fig. 15- Effect of Strengthening Nib Region on response ( $a/d=1.5$ )

Figs. (16) and (17) show that the failure at early stages of loading occurred due to shear failure of the L-shaped CFRP sheets for specimen (NSTR1-A), but with adding the strips, more stiff behavior can be achieved, with some development in ultimate load. Specimen (NSTR1-B) continues to accommodate loading up to the instant when bond failure between the epoxy and concrete occurred. Thus, one may conclude that increasing the L-shaped sheets and the horizontal side strips may results in increasing load capacity considerably.

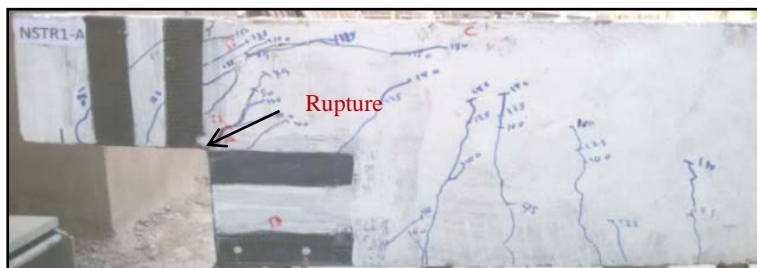


Fig. 16- Cracks Patterns for Strengthening beams NSTR1-A



Fig. 17- Cracks Patterns for Strengthening beams NSTR2-A

7.7 Specimens NSTR1-B & NSTR2-B

These specimens were strengthened at nib region with two different configurations for ( $a/d=1.5$ ) to avoid the failure pattern of specimens (NSTR1-A & NSTR2-A). The specimen (NSTR1-B) was strengthened with three strips in nib region, while the specimen (NSTR2-B) was a trail to improve the strengthening of the specimen (NSTR1-B) by adding three strips with angle  $45^\circ$  at each face to prevent the delamination of CFRP sheets. The details of such configurations are given in Table (11) and shown in Fig. (2).

Comparing the load deflection-curve of such specimens with specimen (NCONT-B), it is obvious that the load capacity increased by about (13.56% and 15%), respectively, stiffer response can be achieved, and the deflection is decreased by about (22.06% and 39.3%), respectively, as shown in Fig. (18).

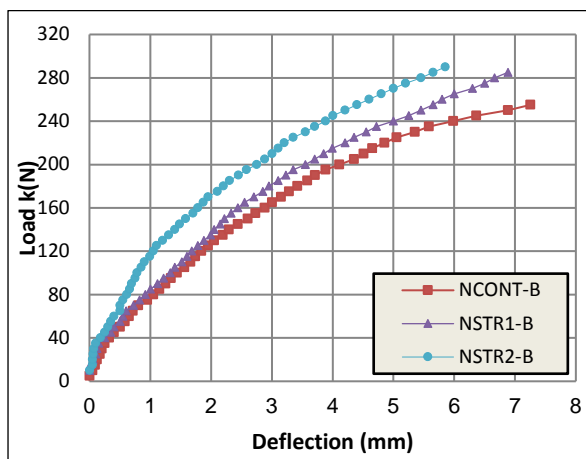


Fig. 18- Effect of Strengthening Nib Region on Response ( $a/d=1.0$ )

It can be concluded the failure mode for the both specimens is determined by a control factor which is the lack of shear resistance in the far zone from the dapped end. Thus, it is expected that the load capacity of the beam may be developed noticeably if enough stirrups are provided in this zone. Also observed, No cracks are developed in dapped end region for beams NSTR1-B (NSTR2-B) up to failure which is the goal of this study, as shown in Figs. (19) and (20).

Comparing Figs.(19) and (20) with crack pattern of specimen (NCONT-B), it can be seen almost few cracks in the extended end of dapped beam. In addition, the failure pattern was changed to diagonal shear failure at mid span of the beam where diagonal tension failure was observed in the extended end for beam (NCONT-B) and cracks not penetrate through CFRP sheet from the loading point towards the far support.



Fig. 19- Crack Patterns for Strengthening beams NSTR1-B



Fig. 20- Crack Patterns for Strengthening beams NSTR2-B

## 8 Conclusions

It found that ( $a/d$ ) ratio has a noticeable effect on behavior of dapped end beam. For the tested reference DEB specimens (with the design steel), an enhancement in failure load by (17%) was observed when adopting shear slenderness ratio of (1.0) instead of (1.5). Furthermore, the failure scenario was observed to be of the type "diagonal tension in the re-entrant corner" instead of "diagonal tension at the nib end". Also, the results revealed that reducing the amount of hanger steel area by a half, led to reducing the capacity by 13% regardless of the shear slenderness ratio( $a/d$ ) this give an

impression that the STM model is conservative relative to the shear friction method and using high strength concrete eliminates to some extent the effect of hanger steel. Whereas, the reduction of nib reinforcement by about (60%), led to drop in failure load about (56%) for  $a/d=1.5$  and (15%) for  $a/d=1.0$ . In addition, it is found that strengthening the nib region with an appropriate arrangement of CFRP strips resulted in initiation of first cracking with higher loading if compared with those non-strengthened specimens. The failure is shifted to occur beyond the point load within the zone that has no shear reinforcement. The crack developed with a reverse orientation and is similar to the diagonal crack in deep beams.

Moreover, It is observed that using CFRP composites in repairing dapped ends contribute in restoring some of the strength that degraded due to deficient reinforcement detailing and improving both of strength and overall response of such elements. The enhancement in strength for specimens repaired at hanger zone by inclined arrangement for shear slenderness ratio of (1.5) was 17% while for  $a/d$  of (1.0), the recovery was about (23%). However, although that the vertical alignment can be done simpler than the inclined form, But the recovery in strength was found to be (11%) for the specimens with large nib end ( $a/d=1.5$ ) and 18% for specimens with  $a/d = 1.0$ . For specimens repaired against the weakness in strength at the nib end, the improvement in strength with shear slenderness ratio ( $a/d$ ) =1.5 was (10%) for the arrangement as L-shaped and horizontal strips. For shear slenderness ratio ( $a/d$ ) of 1.0, the improvement in strength was 15% using the inclined alignment strips. Consequently, It can be seen that alignment method of the strengthening material, play an important role in recovery of the degradation in strength caused due deficiency in steel detailing especially within the disturbed zones of RC members. Thus, It is recommended to use inclined alignment of strengthening material, preferably (45°) as it yields best results if compared with other arrangements and to adopt the low values of shear slenderness ratio (less than or equal 1.0).

## REFERENCES

- [1]- S.K. Liem, Maximum Shear Strength of Dapped-end or Corbel. MSc Thesis, College of Engineering, University Concordia, Montreal, Quebec, Canada, August 1983
- [2]- K.M.P. So, The Behaviour of Thin Stemmed Precast Prestressed Concrete Members with Dapped Ends. Department of Civil Engineering and Applied Mechanics, McGill University, Montreal, Canada, June 1989.
- [3]- S. Ahmad, A. Elahi, J. Hafeez, M. Fawad, Z. Ahsan, Evaluation of the Shear Strength of Dapped Ended Beam. *Life Sci. J.* 3(10) (2013) 1038-1044.
- [4]- A. Atta, M. Taman, Innovative method for strengthening dapped-end beams using an external prestressing technique. *Mater. Struct.* 49(8) (2016) 3005–3019. doi:10.1617/s11527-015-0701-8.
- [5]- A.H. Mattock, T.C. Chan, Design and Behavior of dapped End Beams. *PCI J.* 24(6) (1979) 28-45. doi:10.15554/pci.11011979.28.45
- [6]- Q. Wang, Z. Guo, P.C.J. Hoogenboom, Experimental Investigation on the Shear Capacity of RC Dapped end Beams and Design Recommendations. *Struct. Eng. Mech.* 21(2) (2005) 221- 235. doi:10.12989/sem.2005.21.2.221
- [7]- T. Peng, Influence of Detailing on Response of Dapped End Beams. M. Sc. Thesis. Department of Civil Engineering and Applied Mechanics, McGill University, Montréal, Canada, April 2009.
- [8]- S.E.-D.M.F. Taher, Strengthening of critically designed girders with dapped ends. *P. I. Civil Eng.-Str. B.* 158(2) (2005) 141-152. doi:10.1680/stbu.2005.158.2.141.
- [9]- A.W. Botros, G.J. Klein, G.W. Lucier, S.H. Rizkalla, P. Zia, Dapped ends of prestressed concrete thin-stemmed members : Part 1, experimental testing and behavior. *PCI J.* 62(2) (2017) 61-82.
- [10]- Iraqi specification No. 5, Portland cement. 1984 (In Arabic)
- [11]- Iraqi specification No. 45, Natural Sources for Gravel that is used in concrete and construction. 1984, (In Arabic)
- [12]- EFNARC, Specification and Guidelines for Self-Compacting Concrete. Association House, 99 West Street, Farnham, Surrey, London, UK, February 2002.
- [13]- ASTM C-494/C 494M –01, Standard Specification for Chemical Admixtures for Concrete. Annual Book of American Society for Testing and Materials, 2001.
- [14]- ASTM A 370-05 (2005), Standard Test Method and Definition for Mechanical Testing of Steel Products. Annual Book of ASTM Standards, Vol.01.01, ASTM, Philadelphia, PA.
- [15]- Sika, SikaWrap-301 C, Technical data sheet, 16/1/2015 edition, Sika Corporation.
- [16]- Sika, Sikadur 330, Technical data sheet, 13/6/2006 edition, Sika Corporation.
- [17]- ACI Committee 237R-07, ACI 237R-07 Self-Consolidating Concrete. Farmington Hills, Am Concrete Inst. 2007.